

# Comparison of airborne laser scanning methods for estimating forest structure indicators based on Lorenz curves

Rubén Valbuena, Jari Vauhkonen, Petteri Packalen, Juho Pitkänen, Matti Maltamo

a b s t r a c t

The purpose of this study was to compare a number of state-of-the-art methods in airborne laser scanning (ALS) remote sensing with regards to their capacity to describe tree size inequality and other indicators related to forest structure. The indicators chosen were based on the analysis of the Lorenz curve: Gini coefficient (*GC*), Lorenz asymmetry (*LA*), the proportions of basal area (*BALM*) and stem density (*NSLM*) stocked above the mean quadratic diameter. Each method belonged to one of these estimation strategies: (A) estimating indicators directly; (B) estimating the whole Lorenz curve; or (C) estimating a complete tree list. Across these strategies, the most popular statistical methods for area-based approach (ABA) were used: regression, random forest (RF), and nearest neighbour imputation. The latter included distance metrics based on either RF (NN-RF) or most similar neighbour (MSN). In the case of tree list estimation, methods based on individual tree detection (ITD) and semi-ITD, both combined with MSN imputation, were also studied. The most accurate method was direct estimation by best subset regression, which obtained the lowest cross-validated coefficients of variation of their root mean squared error CV(RMSE) for most indicators: *GC* (16.80%), *LA* (8.76%), *BALM* (8.80%) and *NSLM* (14.60%). Similar figures [CV(RMSE) 16.09%, 10.49%, 10.93% and 14.07%, respectively] were obtained by MSN imputation of tree lists by ABA, a method that also showed a number of additional advantages, such as better distributing the residual variance along the predictive range. In light of our results, ITD approaches may be clearly inferior to ABA with regards to describing the structural properties related to tree size inequality in forested areas.

## 1. Introduction

Indicators describing forest structure can be a valuable support tool in decision-making and forest management planning. Maps of forest structure indicator estimates can be used as a reference to evaluate the success of regeneration groups, plan the location of the next selective cuttings or evaluate the need for thinning (Burger, 2009). Because of its complete three-dimensional charac-

terization of vegetation, airborne laser scanning (ALS) remote sensing allows for evaluating properties related to forest structure in broad forest areas (Lefsky et al., 2005; Maltamo et al., 2005). These properties can be exploited to study forest successional stages (Falkowski et al., 2009; Valbuena et al., 2013a), the risk of wild fire propagation (Andersen et al., 2005; Hall et al., 2005) or wind-throw damage (Suárez et al., 2008), or characteristics related to habitat quality (Lefsky et al., 2002; Martinuzzi et al., 2009).

Lexerød and Eid (2006) pointed out a number of motivations for using indicators derived from Lorenz curves to describe forest structure. In a forest, the Lorenz curve expresses dominance relations by comparing relative cumulated proportions of basal area and stem density accounted for each tree (Valbuena et al., 2012). Gini coefficient (*GC*), Lorenz asymmetry (*LA*), the proportions of basal area (*BALM*) and stem density (*NSLM*) stocked above the quadratic mean diameter, are indicators based on the Lorenz curve

which have been suggested for describing tree size inequality and the balance among forest subpopulations. The GC has been demonstrated to more reliably describe tree size distributions than other indicators based on product moments (Knox et al., 1989) or information theory (Valbuena et al., 2012). For this reason, Bollandsås and Næsset (2007) and Duduman (2011) used GC as a basis to discriminate among differently-shaped diameter distributions. The GC is the ratio between the second and first L-moments, and therefore a second order descriptor of concentration, i.e. relative dispersion (Hosking, 1990). The attention has recently been turned to studying tree size inequality by L-moments, especially with regards to their relations with ALS datasets (Ozdemir and Donoghue, 2013; Valbuena et al., 2013b). Furthermore, the coefficient of LA developed by Damgaard and Weiner (2000) was employed by Valbuena et al. (2013a) for characterizing the relation between dominant and subdominant cohorts in multi-layered forests. LA is a joint description of BALM and NSLM, two important structural characteristics of forests closely related to one another. In forestry practice, BALM and NSLM have traditionally applied when using structural stocking guides in decision-making (Gove, 2004).

Previous research aiming at estimating these indicators from ALS were mainly based on parametric modelling, including best subset (Valbuena et al., 2013b) and beta regression (Valbuena et al., 2013a). Most difficulties were found in the variance structure observed on the prediction, and also on the complexity of the relation of LA with ALS metrics. These issues may be solved when using non-parametric approaches based on nearest neighbour imputation ( $k$ -NN). Maltamo et al. (2006) and Hudak et al. (2008) outlined a number of advantages in using non-parametric procedures, which can make them preferable depending on each application. The method of most similar neighbour (MSN) imputation has already become operational for ALS-estimation of forest variables (Maltamo and Packalen, 2014). Based on a canonical correlation analysis, MSN imputes the  $k$  most similar relations of covariability between response and predictors found within the training dataset (Moeur and Stage, 1995). Furthermore, random forest (RF) is also becoming increasingly popular in ALS remote sensing (Falkowski et al., 2009; McInerney et al., 2010; Yu et al., 2011). RF consists in bootstrapping the training data and computing a regression tree at each iteration, i.e. recursive partitioning by a succession of binary splits of predictor thresholds determined under the criterion of residual sum of squares minimization (Hastie et al., 2009). A combination of RF and  $k$ -NN is an approach where a distance metric used in  $k$ -NN is determined based on RF proximity matrix (NN-RF) (Crookston and Finley, 2008). Hudak et al. (2008) found NN-RF to be more robust than other nearest neighbour methods for imputing species-specific basal area and stem densities. We therefore hypothesised that a similar outcome may be obtained for Lorenz curve descriptors, as they simultaneously describe the relations between basal area and stem density (Valbuena et al., 2012).

These methods can be employed with the purpose of obtaining the estimation of a complete tree list, an alternative which may be beneficial when the interest is on knowing the shape of the diameter distribution, for instance in complex multilayered forest structures. Bollandsås and Næsset (2007) used an area-based approach (ABA) with partial least squares regression to estimate discrete quantiles along the diameter distribution, using the GC as a basis for stratifying the dataset into homologous diameter distribution types. Alternatively, estimating Weibull model parameters allowed inferring diameter distributions presenting a wide range of simple shapes without prior stratification (Gobakken and Næsset, 2004; Maltamo et al., 2007). Maltamo et al. (2006) introduced the use of MSN imputation in ALS estimation, later including the imputation of discrete quantiles (Packalén and Maltamo, 2008), which tolerated the use of complex diameter distribution shapes without theoretical parameterization. Both diameter and basal area-weighted distributions

have been estimated with the intention of improving ALS prediction of forest variables (Gobakken and Næsset, 2004; Maltamo et al., 2007). However, no previous research has been devoted to applying this method on the Lorenz curve, which is a joint description of the intrinsic relation between a diameter distributions and its basal area-weighted (Gove and Patil, 1998; Valbuena et al., 2012).

Individual tree detection (ITD) methods have also traditionally been a source for supplying tree lists. ITD methods are based on segmentation of individual tree crowns from a canopy height model (CHM). The performance of the ITD algorithms typically depends on tree density and spatial distribution of trees, i.e. clustering patterns (Vauhkonen et al., 2012). They usually have the disadvantage of underestimating the understory, although this may not matter for estimating many important forest parameters such as basal area or volume (Persson et al., 2002; Pitkänen et al., 2004). More information on the understory may be obtained with improved tree detection algorithms (Lähivaara et al., 2013), direct point cloud segmentation (Li et al., 2012), using full-waveform ALS information (Reitberger et al., 2009), or analyzing combined leaf-on and leaf-off acquisitions in deciduous forests (Hill and Broughton, 2009). Maltamo et al. (2004), Lindberg et al. (2010), Vauhkonen et al. (2010) and Vastaranta et al. (2012) combined ABA and ITD with the purpose of overcoming this difficulty and improving estimation accuracy. Moreover, Breidenbach et al. (2010) introduced the idea of semi-ITD, in which all trees measured inside a given segment are considered to be represented by that segment, and not just the dominating tree. All these methods have been commonly evaluated by means of the improvement obtained in total forest estimates.

In this article we compare these state-of-the-art ALS estimation methods, with the objective of evaluating them with regards to their capacity for assessing characteristics of forests related to tree size inequality, and the balance between overstorey and understory layers. Indicators derived from the study of the Lorenz curve were selected for this purpose, further clarifying their relations with ALS metrics. We compared the results obtained with three different estimation strategies consisting of: (A) direct indicator estimation; (B) non-parametric estimation of the Lorenz curve, and posterior indicator derivation; or (C) estimating a complete tree list, from which the Lorenz curve and derived indicators were later derived (Fig. 1). Many different methods were tested for each strategy, with the purpose of selecting the most appropriate methodological combination for this type of forest structure-related response.

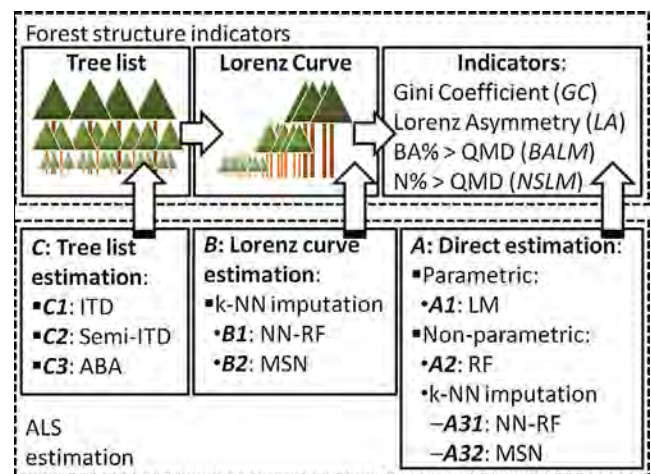


Fig. 1. Flowchart describing the procedure for deriving indicators of forest structure based on Lorenz ordering (above), and how the alternatives considered for their estimation by ALS remote sensing (below) relate to each step of this process. BA: basal area; N: stem density; QMD: quadratic mean diameter; ABA: area-based approach; ITD: individual tree detection; NN: nearest neighbour; RF: random forest; MSN: most similar neighbour; LM: linear model.

## 2. Materials and methods

### 2.1. Study area and remote sensing predictors

The study was carried out in 800 ha of forest situated at the municipality of Kiihtelysvaara in the province of North Karelia (Finland; approx. lat.: 62°31'N; lon.: 30°10'E; 130–150 m above sea level). Main tree species in the area were Scots pine (*Pinus sylvestris* L.) and Norway spruce (*Picea abies* (L.) Karst.), with a minor proportion of broadleaved species. The ALS data were acquired on 26 June 2009, using an ALTM Gemini sensor (Optech, Canada). The flight was performed at a height of about 600 m above terrain level with a maximum scanning angle of 26°, rendering a 320 m swath width with a 55% side lap between strips. A pulse repetition rate of 125 kHz, yielded a high-resolution dataset with nominal scan density of 11.9 pulses m<sup>-2</sup>. Returns were classified as ground by iteratively filtering lower returns into a Delaunay-triangulated irregular network (c.f. Axelsson, 2000). Ground points were interpolated into a digital terrain model (DTM) of 0.5-m pixel size.

By subtracting the DTM value beneath each individual ALS echo, their altitudes above ground level were obtained as a prior step for predictor computation. ALS predictors were moment, order and quantile statistics (Magnussen and Boudewyn, 1998), L-moments and their ratios (Hosking, 1990) and canopy cover metrics (McGaughey, 2012) computed from these ALS echo altitudes. This set of predictors was generated with the assistance of software FUSION (version 3.1, USDA Forest Service), and statistical analyses were carried out in R environment (R Development Core Team, 2011). The initial predictor dataset was reduced using least absolute shrinkage and selection operator (LASSO; Hastie et al., 2009), as detailed in Valbuena et al. (2014). As common in ABA methods, the same metrics were used to estimate them at plot level, for model training, and over a grid of cells covering the whole ALS surveyed area, for wall-to-wall prediction of the target response (Næsset, 2002).

### 2.2. Lorenz curve and forest structure indicators

Field survey was completed between May and June 2010, and consisted of stratified sampling with a total of 79 squared plots whose positions were subjectively determined to assure full coverage of variability range in the forest response. Plot size was either 20 × 20, 25 × 25 or 30 × 30 m, varying in relation to stem density for practical purposes. The forest mensuration campaign determined diameter at breast height ( $dbh_i$ , cm) with a calliper, tree height ( $h_i$ , m) with a Vertex hypsometer (Haglöf UAB, Sweden), and species ( $sp_i$ , dummy variable), for every individual tree ( $i$ ) within plot with either  $dbh_i \geq 5$  or  $h_i \geq 4$ . Stem volumes ( $v_i$ , m<sup>3</sup>) were obtained as detailed by Vauhkonen et al. (2014). The position of every individual tree recorded in the field was determined in relation to the ALS dataset, using the least squares method described by Korpela et al. (2007). Basal areas were calculated for single stems ( $ba_i$ , m<sup>2</sup>), and quadratic mean diameters computed at plot level ( $QMD$ , cm) as the  $dbh$  which corresponds to the mean basal area ( $\bar{ba}$ , m<sup>2</sup>). By ordering the individual trees in ranks ( $r$ ) of decreasing  $dbh$ , the Lorenz curves were computed at plot level as the cumulative proportion of the total basal area  $M(x_r)$  in relation to the cumulative proportion of stem density  $x_r$  accounted from each of them (Valbuena et al., 2012). The indicators of forest structure were all based on this Lorenz curve, using the rationale detailed by Valbuena et al. (2013b).

The first indicator of forest structure was  $GC$ , i.e. the Gini coefficient of the plot level  $dbh$  distribution, also called L-coefficient of variation (Hosking, 1990). The second indicator was  $NSLM$ , the proportion of number of stems which are larger than the weighted mean ( $QMD$ ). In other words,  $NSLM$  is the share of stem density

stocked above the  $QMD$ , which is the value of the Lorenz plot's  $x$ -axis at the inflexion point of the curve  $x_{QMD}$  (Valbuena et al., 2013a). The third indicator was the corresponding value for the  $y$ -axis  $M(x_{QMD})$ , which is the proportion basal area larger than the  $QMD$  ( $BALM$ ; Gove, 2004). It was also considered to average the latter two indicators into a single one describing the skewness of the Lorenz curve. A fourth indicator of Lorenz asymmetry ( $LA$ ) was therefore computed, using the concept developed for forestry by Valbuena et al. (2013a) as modified version of the original indicator designed by Damgaard and Weiner (2000).

It is noteworthy to reflect on the properties of these indicators, with the intention of assisting the readers in interpreting the results of this study. The dependent variables considered are dimensionless indices and proportions, and therefore they all theoretically range [0, 1]. However, this range is in practice limited a number of factors. For instance, the upper limit at  $GC = 1$  (mathematically provided by a maximally bimodal distribution), corresponds to a forest situation which is likely to be ecologically implausible (Valbuena et al., 2013a). Moreover, the quadratic relation between  $dbh_i$  and  $ba_i$  imposes a finite lower limit to the  $QMD$ , and therefore to the probability density of the basal area-weighted distributions (Gove and Patil, 1998). As a result, the theoretical range of values for  $BALM$  and  $NSLM$  is in practice much shorter. For instance, Gove (2004) demonstrated that  $BALM$  has a maximum range between [0.58, 0.99] for any  $dbh$  distribution conforming to a Weibull function, which is a common condition for real forests. A similar situation occurs for  $NSLM$ , as some probability density must always be above the  $QMD$ , and the position of the Lorenz curve's inflexion cannot range the whole extent of the  $x$ -axis in practice. Furthermore, Valbuena et al. (2013b) reflected on the inverse relation between  $BALM$  and  $NSLM$ , which makes them cancel each other out in their averaged  $LA$  indicator, therefore further reducing the plausible range of values for  $LA$ .

### 2.3. Strategies for ALS estimation of Lorenz indicators

With the purpose of predicting the described indicators of forest structure by means of ALS remote sensing, a number of approaches were followed and compared. They all may be grouped in three main types of strategies, as each of them obtained the predictions by either (A) estimating the target indicators directly, (B) estimating the whole Lorenz curve, or (C) estimating a full tree list (Fig. 1). All these approaches are intrinsically related, as the Lorenz curve expresses the quadratic relationship between the  $dbh$  distribution and its area-based weighted counterpart (Gove and Patil, 1998). In strategy A, ALS metrics were related with each response variable  $y_A = \{GC, LA, BALM, NSLM\}$  at plot level. Strategy B consisted in estimating regular quantiles along the whole Lorenz curve  $y_B = \{-M(.05), M(.10), \dots, M(.90), M(.95)\}$ , and use them for deriving the same indicators afterwards. Being  $M(x_r)$  the Lorenz curve of trees ordered by decreasing sizes,  $M(.05)$  is the relative proportion of the total basal area which is stocked in the 5% largest trees,  $M(.10)$  is for the largest 10%, etcetera. Furthermore, methods following strategy C yielded an estimation along the whole  $dbh$  frequency distribution at discrete 1 cm-wide diameter classes. In other words,  $y_C = \{N_{dbh=1}, N_{dbh=2}, \dots, N_{dbh=50}, N_{dbh=51}\}$  where  $N_{dbh=i}$  was the proportion in number of stems for the diameter class  $i$ . The same Lorenz-based indicators were also generated at plot level from these estimated tree lists, and therefore the final outcome of any of these approaches was a final estimate for each indicator

$$\hat{y} = \left( \widehat{GC}, \widehat{LA}, \widehat{BALM}, \widehat{NSLM} \right). \quad (1)$$

All the methods considered were compared by means of their capacity for reliably predicting the targeted final indicators of forest structure. The observed values  $y_j = (GC_j, LA_j, BALM_j, NSLM_j)$  were

computed for each plot  $j = 1, 2, \dots, m$  from the field data. The predicted indicators  $\hat{y}_j = (\widehat{GC}_j, \widehat{LA}_j, \widehat{BALM}_j, \widehat{NSLM}_j)$  were all obtained in a leave-one-out cross validation (LOOCV) fashion, as detailed for each method. Each of these target indicators  $\hat{y}_j$  were also generated from the outcome of those methods aiming at deriving either a Lorenz curve (B) or a *dbh* distribution (C), following the same approach as for the field data. In other words, for the purpose of this study we focused on the capacity of the methods to detect properties related to *dbh* inequality, regardless of their capacity for *dbh* estimation itself. LOOCV procedures involved, in all cases, the full process of indicator generation: training, including both distance metric calculation and imputation (Packalén et al., 2012), and also tree list and Lorenz curve generation. The discrepancy between the observed ( $y_j$ ) and predicted ( $\hat{y}_j$ ) values could therefore be evaluated by their mean difference (bias), and also by their root mean squared error (RMSE). By dividing by the observed mean values, we also obtained relative figures for the bias (bias%), and also the coefficient of variation of the RMSE [CV(RMSE)%]. Coefficients of determination ( $R^2$ ) were also employed to compare the relation between  $y_j$  and  $\hat{y}_j$ , from the sums of squares ratio between residuals ( $y_j - \hat{y}_j$ ) and the total observed variance ( $y_j - \bar{y}_j$ ).

Many different estimation methods were tested for each of these strategies (Fig. 1). The ABA method was employed across all strategies, in the sense of relating ALS metrics at plot level. Best subset regression method based on the linear model (LM) was selected as parametric approach for direct indicator estimation. Non-parametric approaches included random forest (RF) and  $k$ -NN methods. For the latter, two types of distance metrics were considered when computing the nearest neighbours. The most similar neighbour (MSN) method, which computes the distance based on canonical correlation, was the first type. On the other hand, the second type was based on using the RF algorithm for computing the distance metric in the imputation (NN-RF). Finally, MSN imputation was the statistical method involved in all approaches following the strategy C of full tree list estimation, though the reference response differed in each case, as detailed below. Another important difference is that imputation in ABA was done at plot level, whereas in ITD and semi-ITD it was carried out the scale tree crowns (segment level).

### 2.3.1. Area-based approaches (ABA)

**2.3.1.1. Best subset linear model (LM).** Best subset regression was carried out following the methodology described by Valbuena et al. (2013b) for a different study area. A set of models was obtained containing all plausible combinations with a number of  $p = 1, \dots, 5$  predictors. The best model was therefore selected under the criterion of lowest Akaike information criterion, using the version corrected (AICc) for finite samples by Sugiura (1978). This procedure was carried out separately for each response variable  $y = (GC, LA, BALM, NSLM)$ . Accuracy assessment was carried out by LOOCV, so that an estimate for each plot  $j$  was obtained after removing it from the training dataset.

**2.3.1.2. Random Forest (RF).** Boosted recursive partitioning was carried out with the package *randomForest* (version 4.6-7; Liaw and Wiener, 2002). The RF iterations were fitted by regression, so that the variable and threshold for dichotomous split at each node were selected under the criterion of minimum residual sum of squares. All plausible candidate predictors were boosted, i.e. randomly permuted, at each node of the tree. New additive terms (tree branches) kept growing recursively according to an exponential loss function (Hastie et al., 2009). A 0.2 fraction of the remaining predictors was excluded at each iteration, and the out-of-bag error, i.e. the residual measured against the samples that did not appear at each bootstrap, was estimated for the resulting RF. This

successive branching iterated until this out-of-bag error became smaller than the standard error of the minimum error rate of all forests. As a result, each forest consisted of 500 regression trees from which their mode is selected for the final RF imputation, or a random selection from equal modes in case of ambiguity. Accuracy assessment was carried out by LOOCV as well, so that a new RF was trained from each subset after removing one plot  $j$ .

**2.3.1.3. Methods based on  $k$ -NN imputation.** Nearest neighbour methods, i.e. estimation based on computing statistical distance metrics to reference sample plots, were carried out with the package *yalmpute* (version 1.0-18; Crookston and Finley, 2008). The choice of the optimal  $k$  is a compromise between bias and precision in the estimation (Eskelson et al., 2009). We decided to set  $k = 3$ , after observing the evolution of a LOOCV RMSE for increasing  $k$ . The final imputed value was a weighted average of the  $k$  nearest neighbours, according to their distance in the feature space. Accuracy assessment was also done by LOOCV, computing new canonical vectors after removing each plot  $j$ , to avoid its potential effect on the canonical correlation itself (Packalén et al., 2012).

The distance metric used in nearest neighbour determination was calculated following two methods: the random forest algorithm (NN-RF) and the canonical correlation components (MSN). Either method consists in transforming the feature space, i.e. the predictor dataset, with the purpose of maximizing the explained variability against the given response. In order to allow direct comparison, algorithm parameters in NN-RF remained unchanged from those described for RF. Package *randomForest* was therefore used within *yalmpute* (method *randomForest*). Being  $y_B$  a multivariate response, in practice this implies a modification of the RF algorithm for computing a separate random forest for each segment of the Lorenz curve (Crookston and Finley, 2008). Then, the imputation in NN-RF was done based on the RF proximity matrix. In MSN, on the other hand, the imputation was done based on the canonical correlation components (Moeur and Stage, 1995). In Lorenz curve estimation, components are computed for the multivariate response a whole (Valbuena et al., 2014). The weighted average of the  $k$  most similar neighbours was computed according to their distance in the projected canonical correlation space (Packalén and Maltamo, 2008).

The use of canonical correlation analysis to calculate the distance metric for imputation makes the MSN method well suited to situations requiring a multivariate response (Packalén et al., 2012). For this reason, Packalén and Maltamo (2008) included the complete tree list as reference dataset during the imputation, in order to obtain discrete estimates along the whole *dbh* distribution. In this study, we considered the possibility for computing the target forest structure indicators from a MSN-estimated complete list (this method is denoted as ABA withing those in strategy C). Thus, the MSN method for ABA estimation was employed across all strategies, and therefore the difference laid on the response being imputed from the neighbours ( $y_A, y_B$  or  $y_C$ ). Being  $y_C$  a large number of dependent variables that would leave insufficient degrees of freedom for canonical correlation analysis, it was used for imputation stage while the components themselves were computed with  $y = (GC, LA, QMD)$ , as these can suffice to obtain accurate predictions of diameter distributions (Maltamo et al., 2009).

### 2.3.2. Individual tree detection (ITD) and semi-ITD (S-ITD)

While ABA methods used the height above ground distribution of individual ALS returns, the ITD and S-ITD methods were based in a high resolution CHM. The CHM was interpolated to a resolution of 0.5 m by taking the maximum ALS echo altitude within a pixel and filling the pixels that had no ALS hits within their area with a median filtering in local windows of 3 by 3 pixels. Hole pixels,

**Table 1**

Accuracy assessment results for estimation methods based on the strategy of (A) direct indicator estimation (see Fig. 1). LM: linear regression model (A1); RF: random forest (A2); NN-RF: nearest neighbour based on RF (A31); MSN: most similar neighbour (A32).

Method	Gini coefficient (GC)				Lorenz asymmetry (LA)			
	RMSE	CV(RMSE)%	Bias	Bias%	RMSE	CV(RMSE)%	Bias	Bias%
A1: LM	0.076	16.80	$5.56 \cdot 10^{-4}$	0.12	0.053	8.76	$6.45 \cdot 10^{-5}$	0.01
A2: RF	0.105	23.44	$1.57 \cdot 10^{-3}$	0.35	0.056	9.27	$7.40 \cdot 10^{-4}$	0.12
A31: NN-RF	0.130	28.81	$-1.03 \cdot 10^{-1}$	-2.28	0.066	10.87	$5.00 \cdot 10^{-4}$	0.08
A32: MSN	0.100	22.16	$5.10 \cdot 10^{-3}$	1.13	0.078	12.91	$-4.97 \cdot 10^{-3}$	-0.82
	Basal area > QMD (BALM)				Stem density > QMD (NSLM)			
	RMSE	CV(RMSE)%	Bias	Bias%	RMSE	CV(RMSE)%	Bias	Bias%
A1: LM	0.068	8.80	$9.71 \cdot 10^{-5}$	0.12	0.064	14.60	$2.20 \cdot 10^{-5}$	0.01
A2: RF	0.078	10.10	$-2.80 \cdot 10^{-3}$	-0.36	0.076	17.15	$-6.43 \cdot 10^{-4}$	-0.15
A31: NN-RF	0.095	12.30	$2.35 \cdot 10^{-3}$	0.30	0.078	17.86	$6.80 \cdot 10^{-3}$	1.54
A32: MSN	0.093	12.04	$-4.20 \cdot 10^{-3}$	-0.55	0.082	18.64	$-7.92 \cdot 10^{-3}$	-1.79

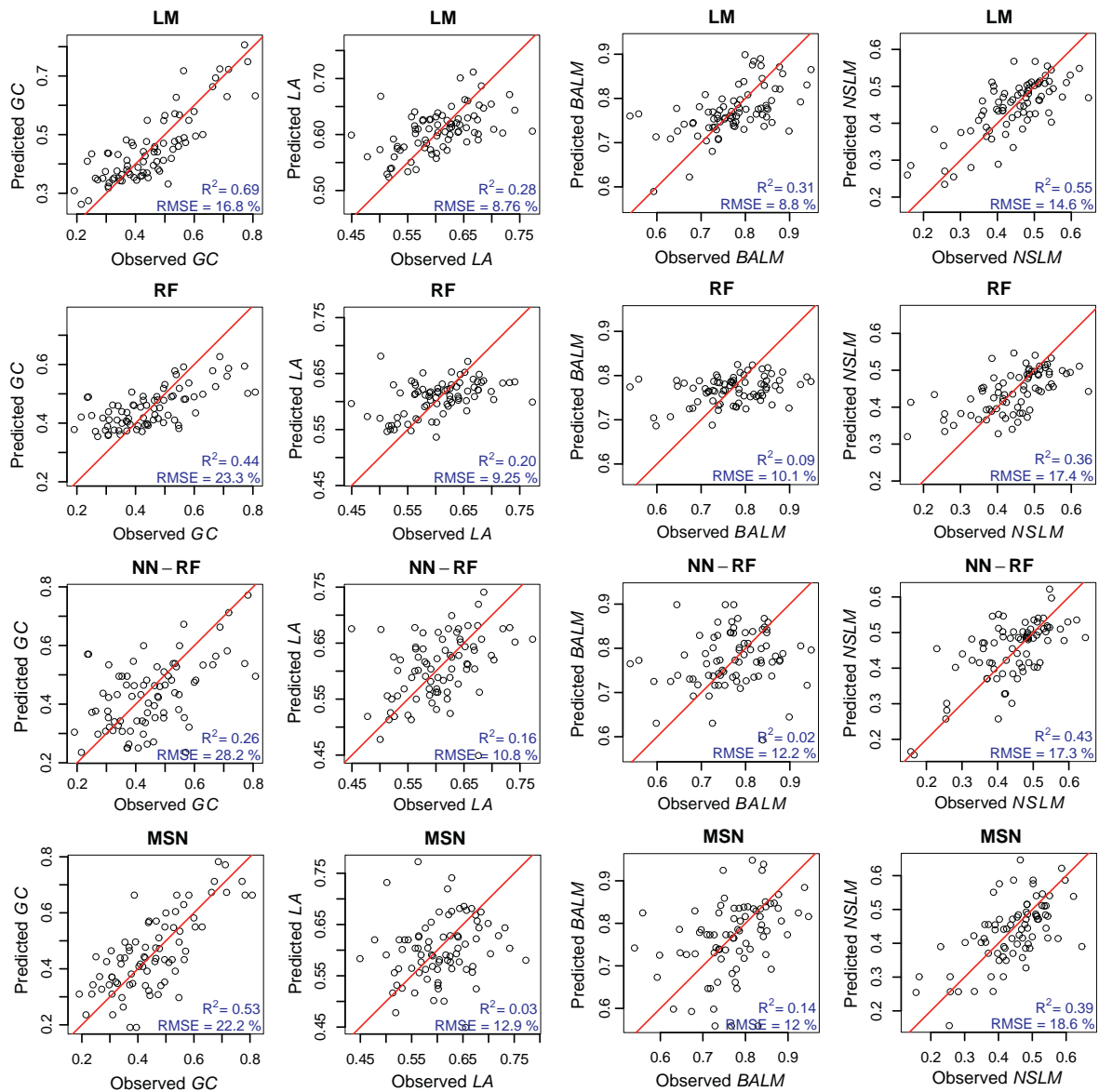


**Fig. 2.** Observed vs. predicted cross-validation plots for estimation methods based on the strategy of (A) direct indicator estimation (see Fig. 1). Each row correspond to an estimation method (Table 1), and columns are distributed by forest response indicator: Gini coefficient (GC), Lorenz asymmetry (LA), and proportions of basal area (BALM) and number of stems (NSLM) larger than the quadratic mean diameter. The line is the 1:1 correspondence between the values observed in the field data and the ALS-predicted values. Coefficients of determination ( $R^2$ ) and coefficients of variation of the RMSE (denoted as RMSE %) are listed for each plot. Table 1 summarizes the RMSEs that correspond to each of these plots.

with at least seven of the eight neighbours exceeding the height value of the centre pixel by more than five meters, were replaced with the median of the values of the neighbour pixels exceeding that threshold.

Segmentation of the CHM into individual tree crowns was based on adaptive filtering (Pitkänen et al., 2004). The CHM was first low-pass filtered using Gaussian kernels with the size of the smoothing window increasing as a function of CHM height. The segments were created around the local maxima using watershed segmentation with a drainage direction following algorithm (Pitkänen, 2005). Pixels lower than two meters were masked out from the crown segments and small segments, at most three pixels in size, were combined to one of the neighbour segments based on the smallest average gradient on the segment boundary between two segments. The method and the applied parameters are described in more detail by Packalén et al. (2013). This single-tree detection algorithm produced altogether 3228 segments when applied to all plots of the study area. The total number of trees measured in the field was 5747, so that the success rate of the algorithm was about 56% on average. Altogether 58% of the segments contained exactly one tree, 39% more than one tree, and 3% were empty. The reader may refer to Vauhkonen et al. (2014) for more details on the outcome obtained by this tree detection method.

The linkage between the resulting ITD segments and the field information was carried out using MSN imputation, as detailed in Vauhkonen et al. (2014). The imputations of both the ITD and S-ITD methods were based on the same segmented data, but the type of the response variable varied. Response variables in the ITD were  $y = (sp_i, dbh_i, h_i, v_i)$  of the largest tree  $i$  per segment. In the S-ITD, species-specific sums of volumes within each segment were used as response variables. The imputations were also carried out in a LOO-CV fashion, i.e. the segments belonging to the same plot  $j$  as the target segment were not available as nearest neighbours, and neither they were involved in the distance metric computation. For all methods involved in strategy C, the resulting estimated tree lists  $\hat{y}_C = \{\hat{N}_{dbh=1}, \hat{N}_{dbh=2}, \dots, \hat{N}_{dbh=50}, \hat{N}_{dbh=51}\}$  were aggregated at plot level into final indicator estimates  $\hat{y} = (\widehat{GC}, \widehat{LA}, \widehat{BALM}, \widehat{NSLM})$ , which were the final results compared against those in strategies A and B.

### 3. Results

#### 3.1. (A) Direct indicator estimation

The first estimation strategy attempted to predict each of the target indicators ( $y_A$ ) directly as univariate response (A; see Fig. 1). Plot level LOOCV results for the resulting LM regression estimation, RF,  $k$ -NN imputations based on RF proximity matrix, and MSN are shown in Table 1. A more detailed evaluation of the predictions can also be assisted by the scatterplots in Fig. 2. The LM best subset regression models (A1) obtained the lowest RMSE and highest  $R^2$  figures in all cases:  $GC$  [ $R^2 = 0.69$ ;  $CV(RMSE) = 16.8\%$ ],  $LA$  [ $R^2 = 0.28$ ;  $CV(RMSE) = 8.6\%$ ],  $BALM$  [ $R^2 = 0.31$ ;  $CV(RMSE) = 8.8\%$ ], and  $NSLM$  [ $R^2 = 0.55$ ;  $CV(RMSE) = 14.6\%$ ]. Moreover, all the LM models were unbiased, and they were found significant in their respective hypothesis testing. The reader may refer to Appendix A for a more detailed description on the best subset regression results.

In the methods based on recursive partitioning (A2 and A31), for all variables the mean squared error stabilized approximately after permuting 200–300 trees, and therefore the fixed number of 500 for the random forest was sufficient. In RF (A2), coefficients of determination were larger for  $GC$  ( $R^2 = 0.44$ ) and  $NSLM$  ( $R^2 = 0.37$ ), than for  $LA$  ( $R^2 = 0.18$ ) and  $BALM$  ( $R^2 = 0.10$ ). As a conse-

quence, the latter indicators showed unsatisfactory observed vs. predicted plots for RF (Fig. 2). This contingency was solved when the RF proximity matrix was used for  $k$ -NN imputation in NN-RF (A31), which clearly partitioned the residual variability more evenly along the full range. RF-NN was therefore more reliable than RF despite of obtaining higher RMSEs.

Comparing the two distance metrics considered for the nearest neighbour methods (A31 and A32), there was not a clear preference as results varied for each type of response. More accurate predictions were obtained with MSN (A32) for  $GC$  [ $CV(RMSE) = 22.2\%$ ], while NN-RF (A31) was preferred in the case of  $LA$  [ $CV(RMSE) = 10.9\%$ ], for instance. In accordance with results obtained with other methods, coefficients of determination were higher in the cases of  $GC$  and  $NSLM$ , than  $LA$  and  $BALM$ . In most cases, methods based on  $k$ -NN imputation showed a more even distribution of residuals along the range of estimation (Fig. 2).

#### 3.2. (B) Lorenz curve estimation

The second estimation strategy consisted in predicting discrete quantiles of the Lorenz curve ( $y_B$ ) as a multivariate response with methods based in nearest neighbour imputation (B; see Fig. 1). Table 2 shows the comparison between the indicators obtained with the field data and those derived from the Lorenz curves estimated by imputation from the rest of plots. In this case, none of the distance metrics was demonstrated clearly superior to the other. The improvement obtained in estimating the whole Lorenz curve (B1 and B2) affected each indicator differently. In the case of  $GC$ , better results were obtained both for NN-RF [ $R^2 = 0.75$ ;  $CV(RMSE) = 15.2\%$ ] and MSN [ $R^2 = 0.65$ ;  $CV(RMSE) = 17.9\%$ ], compared to A31 and A32. In contrast, results for  $LA$  by NN-RF [ $R^2 = 0.06$ ;  $CV(RMSE) = 12.1\%$ ] and MSN [ $R^2 < 0.01$ ;  $CV(RMSE) = 13\%$ ] were worse than those obtained by direct estimation. Observed vs. predicted plots were also obtained in a LOOCV fashion. Both methods showed a tendency to overestimate plots with low  $BALM$  (Fig. 3), which effectively signaled that most uncertainty in the prediction was in the quantiles with higher variability  $M(.05 - .30)$ . This occurred in MSN (B2) as well, despite of z-standardizing the response.

#### 3.3. (C) Tree list estimation

The last estimation strategy consisted in predicting the frequencies at the full range of  $dbh$  classes, therefore producing a complete tree list from which the Lorenz curve was afterwards generated, as if it was the field data itself (C; see Fig. 1). Results obtained for each Lorenz indicator derived at plot level from the resulting tree lists are shown in Table 3 and Fig. 4. The ITD method (C1) notably underestimated  $GC$  (−41.7%) and overestimated  $QMD$  (24.87%). This bias in determining  $QMD$  affected  $BALM$  more severely than  $NSLM$  (Table 3), but the overall underestimation in their averaged  $LA$  demonstrated the ITD method unreliable for predicting the target indicators of forest structure. As it was expected, involving the understorey in the semi-ITD approach (C2) improved the results obtained by ITD. Using S-ITD, RMSEs for  $GC$ ,  $LA$ ,  $BALM$  and  $NSLM$  decreased 54%, 45%, 52% and 28% respectively, compared to ITD. The best advantage was nonetheless to obtain unbiased estimates, hence correcting the ITD underestimations observed for  $GC$  and  $LA$ . In any case, the best results were achieved by ABA, which imputed tree lists directly at the plot level using MSN (C3). ABA for tree list imputation at plot level by MSN also obtained some of the lowest RMSE and highest  $R^2$  figures:  $GC$  [ $R^2 = 0.74$ ;  $CV(RMSE) = 16.1\%$ ],  $LA$  [ $R^2 = 0.15$ ;  $CV(RMSE) = 10.5\%$ ],  $BALM$  [ $R^2 = 0.27$ ;  $CV(RMSE) = 10.9\%$ ], and  $NSLM$  [ $R^2 = 0.60$ ;  $CV(RMSE) = 14.1\%$ ]. Generally speaking, the resulting observed vs. predicted plots showed C3 to be an advantageous approach (Fig. 4).

**Table 2**

Accuracy assessment results for estimation methods based on the strategy of (B) Lorenz curve estimation (see Fig. 1). NN-RF: nearest neighbour based on random forest (B1); MSN: most similar neighbour (B2).

Method	Gini coefficient (GC)				Lorenz asymmetry (LA)			
	RMSE	CV(RMSE)%	Bias	Bias%	RMSE	CV(RMSE)%	Bias	Bias%
B1: NN-RF	0.080	17.83	$-1.06 \cdot 10^{-2}$	-2.36	0.081	13.37	$4.47 \cdot 10^{-4}$	0.07
B2: MSN	0.080	17.86	$-1.73 \cdot 10^{-3}$	-0.38	0.079	13.01	$-1.54 \cdot 10^{-2}$	-2.54
	Basal area > QMD (BALM)				Stem Density > QMD (NSLM)			
	RMSE	CV(RMSE)%	Bias	Bias%	RMSE	CV(RMSE)%	Bias	Bias%
B1: NN-RF	0.087	11.27	$1.39 \cdot 10^{-3}$	0.18	0.093	21.14	$-4.95 \cdot 10^{-4}$	-0.11
B2: MSN	0.087	11.25	$-1.06 \cdot 10^{-2}$	-1.38	0.087	19.79	$-2.01 \cdot 10^{-2}$	-4.56

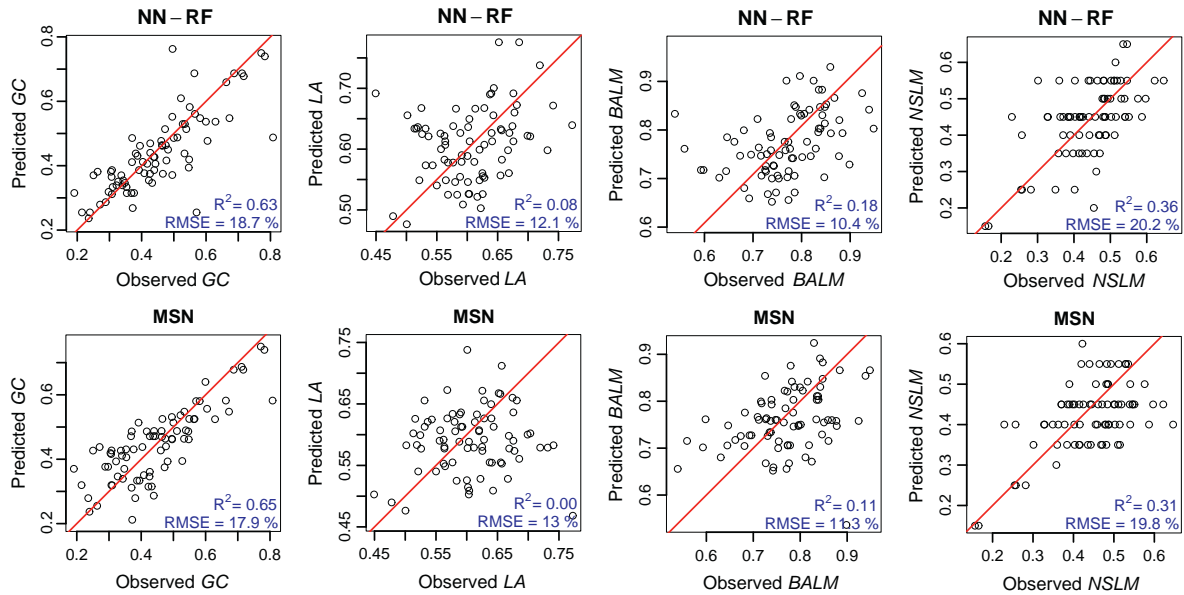


**Fig. 3.** Observed vs. predicted cross-validation plots for estimation methods based on the strategy of (B) Lorenz curve estimation (see Fig. 1). Each row correspond to an estimation method (Table 2), and columns are distributed by forest response indicator: Gini coefficient (GC), Lorenz asymmetry (LA), and proportions of basal area (BALM) and number of stems (NSLM) larger than the quadratic mean diameter. The line is the 1:1 correspondence between the values observed in the field data and the ALS-predicted values. Coefficients of determination ( $R^2$ ) and coefficients of variation of the RMSE (denoted as RMSE) are listed for each plot. Table 2 summarizes the RMSEs that correspond to each of these plots.

## 4. Discussion

### 4.1. Comparing among indicators

A comparison among indicators in terms of the RMSE figures obtained can only be carried out after reflecting on the limits in the dynamic ranges that their values can obtain in real forests (see Section 2.2). The easiest way is to keep in mind the empirical standard deviations observed in the training dataset, which were 0.137 for GC, 0.063 for LA, 0.082 for BALM, and 0.097 for NSLM. Any comparison by RMSE and bias must account for this difference, as the larger practical range of values for GC makes this indicator more prone to relative errors than e.g. LA. On the other hand, this property also makes GC more likely to obtain higher coefficients of determination  $R^2$ . Considering, for instance, that BALM and NSLM present similar empirical variability, the former was notably more feasible to be determined by ALS remote sensing. A reason explaining this effect may be the fact that ALS metrics often have more explanatory power for forest variables dependent on basal area than those related to stem density (Næsset, 2002; Lefsky et al., 2005). Overall, obtaining reliable estimations was demonstrably possible for all the indicators considered, and therefore selecting the appropriate indicator of forest structure depends more on the

purpose and target forest properties than for their relation to ALS metrics.

### 4.2. Comparing among statistical methods

All the statistical methods considered obtained statistically sound results in terms of their RMSEs and, therefore, a number of other reasons for choosing either one may be pointed out. Highest accuracy figures in the prediction were obtained by LM regression (A1), which was not surprising as this method minimized squared residuals directly for each the target indicator. However, it can be observed in Fig. 2 that the residual variance followed a pattern of underestimating high values of GC and LA, and overestimating low ones. On the other hand, the residual variance was more evenly distributed along the dynamic range of each indicator when methods based on direct  $k$ -NN imputation, which may therefore be preferred in such case.

RF did not seem to render special advantages for direct indicator estimation, except in the case of LA, for which accuracies obtained in A2 were comparable to those for LM (A1). The reason for this may be the complexity of the LA indicator, as Valbuena et al. (2013b) found its separate components – namely BALM and NSLM – to have relations with several ALS metrics of opposite signs

**Table 3**  
Accuracy assessment results for estimation methods based on the strategy of (C) tree list estimation (see Fig. 1). ITD: individual tree detection (C1); S-ITD: semi-ITD (C2); ABA: MSN tree list estimation at plot level (C3).

Method	Gini coefficient (GC)				Lorenz Asymmetry (LA)			
	RMSE	CV(RMSE)%	Bias	Bias%	RMSE	CV(RMSE)%	Bias	Bias%
C1: ITD	0.213	47.26	$-1.88 \cdot 10^{-1}$	-41.77	0.110	18.13	$-6.86 \cdot 10^{-2}$	-11.32
C2: S-ITD	0.098	21.75	$8.76 \cdot 10^{-3}$	1.95	0.060	9.86	$-2.91 \cdot 10^{-3}$	-0.48
C3: ABA	0.072	16.09	$-1.28 \cdot 10^{-2}$	-2.85	0.064	10.49	$-2.01 \cdot 10^{-2}$	-3.31
	Basal area > QMD (BALM)				Stem Density > QMD (NSLM)			
	RMSE	CV(RMSE)%	Bias	Bias%	RMSE	CV(RMSE)%	Bias	Bias%
C1: ITD	0.178	23.07	$-1.47 \cdot 10^{-1}$	-19.12	0.095	21.47	$1.02 \cdot 10^{-2}$	2.31
C2: S-ITD	0.086	11.16	$1.62 \cdot 10^{-3}$	0.21	0.069	15.57	$-7.44 \cdot 10^{-3}$	-1.69
C3: ABA	0.084	10.93	$-2.49 \cdot 10^{-2}$	-3.23	0.062	14.07	$-1.53 \cdot 10^{-2}$	-3.46

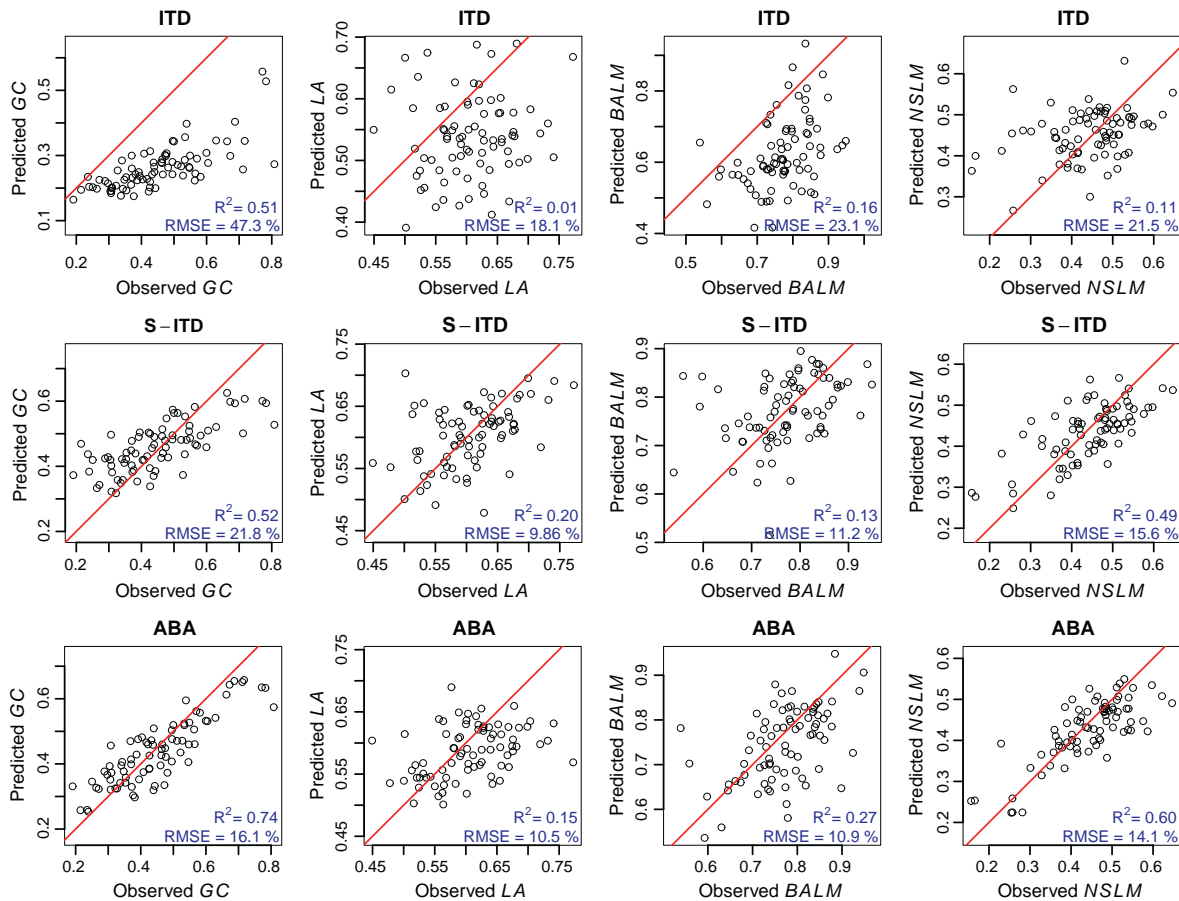


**Fig. 4.** Observed vs. predicted cross-validation plots for estimation methods based on the strategy of (C) tree list estimation (see Fig. 1). Each row correspond to an estimation method (Table 3), and columns are distributed by forest response indicator: Gini coefficient (GC), Lorenz asymmetry (LA), and proportions of basal area (BALM) and number of stems (NSLM) larger than the quadratic mean diameter. The line is the 1:1 correspondence between the values observed in the field data and the ALS-predicted values. Coefficients of determination ( $R^2$ ) and coefficients of variation of the RMSE (denoted as RMSE) are listed for each plot. Table 3 summarizes the RMSEs that correspond to each of these plots.

(either direct or indirect). In such type of cases, recursive partitioning may allow to express the relations of ALS metrics against each of those components, explaining different portions of variance separately at different branches of a regression tree (Hastie et al., 2009). This may also explain why direct estimation of LA was one of the few cases in which NN-RF estimation was more accurate than MSN. Otherwise, the generality was for MSN to outperform NN-RF. This result differs from those obtained by Hudak et al. (2008) for other type of forest variables. On the other hand, Packalén et al. (2012) found NN-RF to perform better than MSN

for univariate responses, while the latter was more beneficial in the multivariate case.

#### 4.3. Comparing among estimation strategies

In principle, direct indicator estimation (strategy A) can be, by definition, expected to obtain the lowest RMSE figures across all methodologies compared. However, tree list estimation by MSN from ALS metrics obtained at plot level was demonstrably beneficial with regards to estimating some of the indicators of for-



est structure considered in this study. This can happen if the application of a given study benefits from having detailed information on the entire diameter distribution (Gobakken and Næsset, 2004; Maltamo et al., 2007). This seems to be the case for the structural indicators selected. Additionally, many stand attributes, such as basal area, number of stems, volume, or timber assortments and their value (Vauhkonen et al., 2014), can be flexibly calculated from the same tree list model which is constructed for the purpose of forest structure characterization. When comparing the MSN estimation, which was common for all strategies, RMSE results obtained in tree list estimation (C3) improved those obtained by Lorenz curve estimation (B2) and direct indicator estimation (A32), generally speaking. Consequently, the results presented in this article may reveal that approaches for tree list estimation (strategy C) could as well be advantageous in describing tree size inequality and the balance between understory and overstory.

The strategy of estimating the whole Lorenz curve (B; Fig. 1) obtained accuracies in between the other two. No benefit was observed in comparison to estimating its corresponding diameter distribution, and therefore strategy C is preferred. One reason can be an accumulation of methodological errors, for instance when splitting the continuous Lorenz curve into discrete quantiles, or while retrieving the curve's inflexion point. Further research could consider using narrower bin sizes, or predicting basal area-weighted and unweighted distributions simultaneously (Gobakken and Næsset, 2004; Maltamo et al., 2007), in pursuit of the final Lorenz curve. In light of these results, there is no interest in estimating the full Lorenz curve when pursuing a prediction of target indicators. There may, however, still be interest in studying the canonical components themselves (e.g. Lefsky et al., 2005), as they can provide with information on the importance of different ALS metrics at diverse portions of the Lorenz curve, therefore relating them to relations among vertical strata (Valbuena et al., 2014).

#### 4.4. Individual tree detection vs. area-based estimation

The adaptive filtering used for ITD was devoted to detecting the presence of small trees as well as large ones, as the amplitude of the filter was roughly proportional to crown size at different tree layers (Pitkänen et al., 2004). In spite of this, the results obtained with ITD were negatively biased for GC (Table 3). Thus, understory ingrowth below the dominant canopy remained undetected, and hence tree size inequality was clearly underestimated. The underestimation in LA also revealed that understory trees are more likely missed when they are smaller (Valbuena et al., 2013a). When the interpretation is based on 2.5-dimensional CHMs, small trees are inherently missed when overtopped by larger ones (Vauhkonen et al., 2012). Although Vauhkonen et al. (2014) showed that this affected only to 13% of the total stem volume, the effect on forest structure indicators is clearly higher. The relatively low rate of success in tree detection for the specific the method employed, and the fact that failure in tree detection happened with higher probability on suppressed trees than dominant ones, led to underestimated tree size inequality. Thus the success achieved by semi-ITD, which improved the ITD results by simply accounting for all the trees enclosed within a segment, is logical and expected. Our results, however, do not preclude other ITD methods with higher tree detection rates of success to obtain better estimations of forest structure indicators. Further research could therefore consider other ITD techniques, such as those based on point segmentation (Li et al., 2012).

Plot level imputation of tree lists following the ABA method obtained the lowest RMSEs for most indicators among all the tree list methods tested (Table 3). This may indicate that segmenting and interpreting a 2.5-dimensional CHM burdens the evaluation of structural properties from forests. However, this was not the

case for LA, a result we found most intriguing. Also Vastaranta et al. (2012) found that the preference for either ABA or ITD may depend on the target forest response. The reason may be grounded on the fact that LA is an indicator on the relative relationships between over and understory both in terms of stem density and basal area (Valbuena et al., 2013b). Consequently, although semi-ITD seemed insufficiently reliable for determining tree size inequality (GC), it can provide a reasonable idea on the relations of dominance among individual trees in multilayered forests. However, we found that computing ALS metrics at the plot level to be more informative than using CHM segments, in terms of the indicators chosen. We therefore recommend the use of ABA above ITD when analyzing structural properties of complex diameter distributions, unless the purpose of a given study requires the detail given at tree crown scale, e.g. research on individual tree competition.

#### 4.5. Effect of scale in estimation of Lorenz-based indicators

The effect of scale on the Lorenz indicators considered was one important issue already mentioned in Valbuena et al. (2013a). As this study was carried out using plots differing in size, there could be a potential small influence of the scale on the results. However, as plot size was determined according to stand density, the number of trees included at each of them can be considered roughly similar. Therefore, even though the 79 cases used for these estimations differ in plot area, they are equal in terms of sample size. Moreover, the scale used also affects different ALS metrics in a dissimilar way, and it is not clear whether these effects are synergetic for the Lorenz indicators and the ALS metrics, affecting the estimation itself. In any case, for the purpose of this study we have considered it to be small effect affecting equally across all the methods and strategies considered. Whether these indicators are more affected by the scale or the sample size, or this effect is also affecting the ALS estimation of Lorenz indicators, are questions to be clarified in future research.

## 5. Conclusions

Results were statistically sound for all the methods based on ABA, and therefore the choice of method may depend more on the properties of the outcoming estimates, such as the distribution of the residual variance. When MSN imputation was used to compute an entire diameter distribution, the accuracy of the resulting indicators was higher than when estimating the Lorenz curve or approaching those same indicators directly. Therefore, tree list estimation can be of interest in studies focused on the structural properties of forests. Lorenz curve estimation may be advanta-

**Table A1**  
Description of metrics computed from ALS return heights (see McGaughey, 2012).

Predictor	Description
P05	5th percentile
P70	70th percentile
L.CV	L-coefficient of variation (ratio between second and first L-moments)
L4	Fourth L-moment
MAD.median	Median absolute deviation from the median
Skew	Third product moment (skewness)
Cover	Percentage of all returns above a height threshold of 1 m
Cover.mode	Percentage of all returns above their mode
Cover.f.mode	Percentage of first returns above their mode
Cover.mean/f	Ratio between the percentage of all returns above their mean and the total number of first returns, in percentage
Cover.mode/f	Ratio between the percentage of all returns above their mode and the total number of first returns, in percentage

**Table A2**

Summary of results for regression estimates and their hypothesis testing.

Regression coefficient	Gini coefficient (GC)				Lorenz asymmetry (LA)			
	Estimate	SE	t-Student	p-value	Estimate	SE	t-Student	p-value
$\beta_0$	-3.10	0.39	-7.89	<0.001***	0.71	$6.61 \cdot 10^{-2}$	10.77	<0.001***
$\beta_1$	5.44	0.45	11.95	<0.001***	-0.20	$3.20 \cdot 10^{-2}$	-6.52	<0.001***
$\beta_2$	2.32	0.73	3.16	0.002**	$-7.88 \cdot 10^{-3}$	$2.89 \cdot 10^{-3}$	-2.73	0.008*
$\beta_3$	$3.91 \cdot 10^{-2}$	$3.00 \cdot 10^{-3}$	13.08	<0.001***	$-9.61 \cdot 10^{-4}$	$4.80 \cdot 10^{-4}$	-2.00	0.048*
$\beta_4$	$-5.90 \cdot 10^{-2}$	$9.08 \cdot 10^{-3}$	-6.50	<0.001***				
$\beta_5$	$4.16 \cdot 10^{-2}$	$9.21 \cdot 10^{-3}$	4.51	<0.001***				
	$R^2$ adj.	RSE	F-Fisher	p-value	$R^2$ adj.	RSE	F-Fisher	p-value
	0.72	$7.24 \cdot 10^{-2}$	41.47	<0.001***	0.34	$5.13 \cdot 10^{-2}$	14.39	<0.001***
	Basal area > QMD (BALM)				Stem density > QMD (NSLM)			
	Estimate	SE	t-Student	p-value	Estimate	SE	t-Student	p-value
$\beta_0$	1.14	0.25	4.61	<0.001***	0.32	0.19	1.72	0.089*
$\beta_1$	-0.38	$6.95 \cdot 10^{-2}$	-5.41	<0.001***	$7.11 \cdot 10^{-3}$	$2.73 \cdot 10^{-3}$	2.61	0.011*
$\beta_2$	$-1.75 \cdot 10^{-2}$	$5.15 \cdot 10^{-3}$	-3.39	<0.001***	$-1.19 \cdot 10^{-2}$	$1.24 \cdot 10^{-3}$	-9.62	<0.001***
$\beta_3$	0.29	$4.74 \cdot 10^{-2}$	6.17	<0.001***	$1.17 \cdot 10^{-2}$	$2.30 \cdot 10^{-3}$	3.92	<0.001***
$\beta_4$	$1.19 \cdot 10^{-2}$	$2.03 \cdot 10^{-3}$	5.56	<0.001***	$1.10 \cdot 10^{-2}$	$1.63 \cdot 10^{-3}$	6.74	<0.001***
$\beta_5$	$-1.16 \cdot 10^{-2}$	$3.34 \cdot 10^{-3}$	-3.48	<0.001***	$8.21 \cdot 10^{-3}$	$1.28 \cdot 10^{-3}$	-6.42	<0.001***
	$R^2$ adj.	RSE	F-Fisher	p-value	$R^2$ adj.	RSE	F-Fisher	p-value
	0.37	$6.48 \cdot 10^{-2}$	10.44	<0.001***	0.59	$5.13 \cdot 10^{-2}$	23.70	<0.001***

SE: standard error. RME: residual standard error.  $R^2$ adj.: coefficient of determination adjusted by degrees of freedom. Levels of significance:NS = not significant ( $p$ -value > 0.05).

\* &lt;0.01.

\* &lt;0.05.

\*\* &lt;0.01.

\*\*\* &lt;0.001.

geous if interested in a deeper exploration on the relations of dominance among canopy strata, but not for indicator estimation. Finally, although the semi-ITD approach may correct the biasing underestimation of tree size inequality obtained by ITD, any approach involving CHM segmentation was demonstrably inferior to plot level training, with regards to estimating forest structure indicators based on the Lorenz curve.

## Acknowledgments

Rubén Valbuena's work was funded by Metsähallitus Grant and the Foundation for European Forest Research (FEFR). This study was also partly funded by the strategic funding of the University of Eastern Finland.

## Appendix A. Detail on results for best subset selection models (LM)

In regression modelling, the selection of independent variables was carried out by imposing a maximum number of five predictors and the criterion of lowest AICc. The resulting models obtained AICc values of -181.32, -238.36, -198.85 and -206.18 respectively for GC, LA, BALM and NSLM. It is worth noting that this criteria yielded best subset models with five predictors, except in the case of LA which included only three. These final models were:

$$GC = \beta_0 + \beta_1 \cdot L.CV + \beta_2 \cdot P05 + \beta_3 \cdot Cover + \beta_4 \cdot Cover.mode + \beta_5 \cdot Cover.f.mode \quad (A.1)$$

$$LA = \beta_0 + \beta_1 \cdot L4 + \beta_2 \cdot MAD.median + \beta_3 \cdot Cover.mode/f \quad (A.2)$$

$$BALM = \beta_0 + \beta_1 \cdot L4 + \beta_2 \cdot MAD.median + \beta_3 \cdot Skew + \beta_4 \cdot Cover + \beta_5 \cdot Cover.f.mode \quad (A.3)$$

$$NSLM = \beta_0 + \beta_1 \cdot P70 + \beta_2 \cdot Cover + \beta_3 \cdot Cover.mode + \beta_4 \cdot Cover.mean/f + \beta_5 \cdot Cover.mode/f \quad (A.4)$$

Table A1 includes a legend explaining these predictors, whereas Table A2 lists the regression estimates and results of hypothesis testing.

## References

- Andersen, H., McGaughey, R.J., Reutebuch, S.E., 2005. Estimating forest canopy fuel parameters using LIDAR data. *Remote Sens. Environ.* 94 (4), 441–449.
- Axelsson, P., 2000. DEM Generation from laser scanner data using adaptive TIN models. *Int. Arch. Photogramm. Remote Sens.* 33 (Part B4), 110–117.
- Bollandsås, O.M., Næsset, E., 2007. Estimating percentile-based diameter distributions in uneven-sized Norway spruce stands using airborne laser scanner data. *Scand. J. For. Res.* 22 (1), 33–47.
- Breidenbach, J., Næsset, E., Lien, V., Gobakken, T., Solberg, S., 2010. Prediction of species specific forest inventory attributes using a nonparametric semi-individual tree crown approach based on fused airborne laser scanning and multispectral data. *Remote Sens. Environ.* 114 (4), 911–924.
- Burger, J.A., 2009. Management effects on growth, production and sustainability of managed forest ecosystems: past trends and future directions. *Forest Ecol. Manage.* 258 (10), 2335–2346.
- Crookston, N.L., Finley, A.O., 2008. Yalmpute: an R package for  $\kappa$ NN imputation. *J. Stat. Softw.* 23 (10), 1–16.
- Damgaard, C., Weiner, J., 2000. Describing inequality in plant size or fecundity. *Ecology* 81 (4), 1139–1142.
- Duduman, G., 2011. A forest management planning tool to create highly diverse uneven-aged stands. *Forestry* 84 (3), 301–314.
- Eskelson, B.N.L., Temesgen, H., Lemay, V., Barrett, T.M., Crookston, N.L., Hudak, A.T., 2009. The roles of nearest neighbor methods in imputing missing data in forest inventory and monitoring databases. *Scand. J. For. Res.* 24 (3), 235–246.
- Falkowski, M.J., Evans, J.S., Martinuzzi, S., Gessler, P.E., Hudak, A.T., 2009. Characterizing forest succession with lidar data: an evaluation for the Inland Northwest, USA. *Remote Sens. Environ.* 113 (5), 946–956.
- Gobakken, T., Næsset, E., 2004. Estimation of diameter and basal area distributions in coniferous forest by means of airborne laser scanner data. *Scand. J. Forest Res.* 19 (6), 529–542.
- Gove, J.H., 2004. Structural stocking guides: a new look at an old friend. *Can. J. Forest Res.* 34 (5), 1044–1056.
- Gove, J.H., Patil, G.P., 1998. Modeling the basal area-size distribution of forest stands: a compatible approach. *Forest Sci.* 44 (2), 285–297.
- Hall, S.A., Burke, I.C., Box, D.O., Kaufmann, M.R., Stoker, J.M., 2005. Estimating stand structure using discrete-return lidar: an example from low density, fire prone ponderosa pine forests. *Forest Ecol. Manage.* 208 (1–3), 189–209.
- Hastie, T., Tibshirani, R., Friedman, J.H., 2009. *The Elements of Statistical Learning. Data Mining, Inference, and Prediction.* Springer, New York.
- Hill, R.A., Broughton, R.K., 2009. Mapping the understorey of deciduous woodland from leaf-on and leaf-off airborne LiDAR data: a case study in lowland Britain. *ISPRS J. Photogramm. Remote Sens.* 64 (2), 223–233.

- Hosking, J.R.M., 1990. L-Moments: analysis and estimation of distributions using linear combinations of order statistics. *J. R. Stat. Soc. Ser. B (Methodological)* 52 (1), 105–124.
- Hudak, A.T., Crookston, N.L., Evans, J.S., Hall, D.E., Falkowski, M.J., 2008. Nearest neighbor imputation of species-level, plot-scale forest structure attributes from LiDAR data. *Remote Sens. Environ.* 112 (5), 2232–2245.
- Knox, R.G., Peet, R.K., Christensen, N.L., 1989. Population dynamics in loblolly pine stands: changes in skewness and size inequality. *Ecology* 70 (4), 1153–1167.
- Korpela, I., Tuomola, T., Välimäki, E., 2007. Mapping forest plots: an efficient method combining photogrammetry and field triangulation. *Silva Fenn.* 41 (3), 457–469.
- Lähivaara, T., Seppänen, A., Kaipio, J.P., Vauhkonen, J., Korhonen, L., Tokola, T., Maltamo, M., 2013. Bayesian approach to tree detection based on airborne laser scanning data. *IEEE Trans. Geosci. Remote Sens.* 52 (5), 2690–2699.
- Lefsky, M.A., Cohen, W.B., Parker, G.G., Harding, D.J., 2002. Lidar remote sensing for ecosystem studies. *Bioscience* 52 (1), 19–30.
- Lefsky, M.A., Hudak, A.T., Cohen, W.B., Acker, S.A., 2005. Patterns of covariance between forest stand and canopy structure in the Pacific Northwest. *Remote Sens. Environ.* 95 (4), 517–531.
- Lexerød, N.L., Eid, T., 2006. An evaluation of different diameter diversity indices based on criteria related to forest management planning. *Forest Ecol. Manage.* 222 (1), 17–28.
- Li, W., Guo, Q., Jakubowski, M., Kelly, M., 2012. A new method for segmenting individual trees from the lidar point cloud. *Photogramm. Eng. Remote Sens.* 78, 75–84.
- Liaw, A., Wiener, M., 2002. Classification and regression by randomForest. *R News* 2 (3), 18–22.
- Lindberg, E., Holmgren, J., Olofsson, K., Wallerman, J., Olsson, H., 2010. Estimation of tree lists from airborne laser scanning by combining single-tree and area-based methods. *Int. J. Remote Sens.* 31 (5), 1175–1192.
- Magnussen, S., Boudewyn, P., 1998. Derivations of stand heights from airborne laser scanner data with canopy-based quantile estimators. *Can. J. Forest Res.* 28 (7), 1016–1031.
- Maltamo, M., Packalén, P., 2014. Species specific management inventory in Finland. In: Maltamo, M., Næsset, E., Vauhkonen, J. (Eds.), *Forestry Applications of Airborne Laser scanning: Concepts and Case Studies. Managing Forest Ecosystems*, vol. 27. Springer, Dordrecht.
- Maltamo, M., Eerikäinen, K., Pitkänen, J., Hyypä, J., Vehmas, M., 2004. Estimation of timber volume and stem density based on scanning laser altimetry and expected tree size distribution functions. *Remote Sens. Environ.* 90 (3), 319–330.
- Maltamo, M., Packalén, P., Yu, X., Eerikäinen, K., Hyypä, J., Pitkänen, J., 2005. Identifying and quantifying structural characteristics of heterogeneous boreal forests using laser scanner data. *Forest Ecol. Manage.* 216 (1), 41–50.
- Maltamo, M., Malinen, J., Packalén, P., Suvanto, A., Kangas, J., 2006. Nonparametric estimation of stem volume using airborne laser scanning, aerial photography, and stand-register data. *Can. J. Forest Res.* 36 (2), 426–436.
- Maltamo, M., Suvanto, A., Packalén, P., 2007. Comparison of basal area and stem frequency diameter distribution modelling using airborne laser scanner data and calibration estimation. *Forest Ecol. Manage.* 247 (1–3), 26–34.
- Maltamo, M., Næsset, E., Bollandsås, O.M., Gobakken, T., Packalén, P., 2009. Non-parametric prediction of diameter distributions using airborne laser scanner data. *Scand. J. Forest Res.* 24 (6), 541–553.
- Martinuzzi, S., Vierling, L.A., Gould, W.A., Falkowski, M.J., Evans, J.S., Hudak, A.T., et al., 2009. Mapping snags and understory shrubs for a LiDAR-based assessment of wildlife habitat suitability. *Remote Sens. Environ.* 113 (12), 2533–2546.
- McGaughey, R.J., 2012. FUSION/LDV: Software for LIDAR Data Analysis and Visualization. Version 3.10. Pacific Northwest Research Station. USDA Forest Service, Seattle, WA.
- McInerney, D.O., Suarez-Minguez, J., Valbuena, R., Nieuwenhuis, M., 2010. Forest canopy height retrieval using LiDAR data, medium-resolution satellite imagery and kNN estimation in Aberfoyle, Scotland. *Forestry* 83 (2), 195–206.
- Moeur, M., Stage, A.R., 1995. Most similar neighbor: an improved sampling inference procedure for natural resource planning. *Forest Sci.* 41 (2), 337–359.
- Næsset, E., 2002. Predicting forest stand characteristics with airborne scanning laser using a practical two-stage procedure and field data. *Remote Sens. Environ.* 80 (1), 88–99.
- Ozdemir, I., Donoghue, D.N.M., 2013. Modelling tree size diversity from airborne laser scanning using canopy height models with image texture measures. *Forest Ecol. Manage.* 295 (1), 28–37.
- Packalén, P., Maltamo, M., 2008. Estimation of species-specific diameter distributions using airborne laser scanning and aerial photographs. *Can. J. Forest Res.* 38 (7), 1750–1760.
- Packalén, P., Temesgen, H., Maltamo, M., 2012. Variable selection strategies for nearest neighbor imputation methods used in remote sensing based forest inventory. *Can. J. Remote Sens.* 38 (5), 557–569.
- Packalén, P., Vauhkonen, J., Kallio, E., Peuhkurinen, J., Pitkänen, J., Pippuri, I., Strunk, J., Maltamo, M., 2013. Predicting the spatial pattern of trees with airborne laser scanning. *Int. J. Remote Sens.* 34 (14), 5154–5165.
- Persson, A., Holmgren, J., Söderman, U., 2002. Detecting and measuring individual trees using an airborne laser scanner. *Photogramm. Eng. Remote Sens.* 68 (9), 925–932.
- Pitkänen, J., 2005. A multi-scale method for segmentation of trees in aerial images. In: Hobbestad, K., (Ed.). In: *Proceedings of the SNS-meeting at Sjusjøen – Forest Inventory and Planning in Nordic Countries. NIJOS-report 09/05*, Norwegian Institute of Land Inventory, Oslo, Norway.
- Pitkänen, J., Maltamo, M., Hyypä, J., Yu, X., 2004. Adaptive methods for individual tree detection on airborne laser based canopy height model. *Int. Arch. Photogramm., Remote Sens. Spatial Inform. Sci.* 36 (Part 8/W2), 187–191.
- R Development Core Team, 2011. *R: A Language and Environment for Statistical Computing*.
- Reitberger, J., Schnörr, C., Krzystek, P., Stilla, U., 2009. 3D segmentation of single trees exploiting full waveform LIDAR data. *ISPRS J. Photogramm. Remote Sens.* 64 (6), 561–574.
- Suárez, J.C., García, R., Gardiner, B.A., Patenaude, G., 2008. The estimation of wind risk in forest stands using ALS. *J. Forest Plann.* 13 (Silvilaser Special Issue), 165–186.
- Sugiura, N., 1978. Further analysts of the data by akaike' s information criterion and the finite corrections. *Commun. Stat. – Theory Methods* 7 (1), 13–26.
- Valbuena, R., Packalén, P., Martín-Fernández, S., Maltamo, M., 2012. Diversity and equitability ordering profiles applied to study forest structure. *Forest Ecol. Manage.* 276, 185–195.
- Valbuena, R., Packalén, P., Mehtätalo, L., García-Abril, A., Maltamo, M., 2013a. Characterizing forest structural types and Shelterwood dynamics from Lorenz-based indicators predicted by airborne laser scanning. *Can. J. Forest Res.* 43 (11), 1063–1074.
- Valbuena, R., Maltamo, M., Martín-Fernández, S., Packalén, P., Pascual, C., Nabuurs, G.J., 2013b. Patterns of covariance between airborne laser scanning metrics and Lorenz curve descriptors of tree size inequality. *Can. J. Remote Sens.* 39 (S1), S18–S31.
- Valbuena, R., Packalén, P., Tokola, T., Maltamo, M., 2014. Canonical correlation analysis for interpreting relations of airborne laser scanning metrics along the Lorenz curve of tree size inequality. *Baltic Forestry* 20 (2) (in press).
- Vastaranta, M., Kankare, V., Holopainen, M., Yu, X., Hyypä, J., Hyypä, H., 2012. Combination of individual tree detection and area-based approach in imputation of forest variables using airborne laser data. *ISPRS J. Photogramm. Remote Sens.* 67 (1), 73–79.
- Vauhkonen, J., Korpela, I., Maltamo, M., Tokola, T., 2010. Imputation of single-tree attributes using airborne laser scanning-based height, intensity, and alpha shape metrics. *Remote Sens. Environ.* 114 (6), 1263–1276.
- Vauhkonen, J., Ene, L., Gupta, S., Heinzel, J., Holmgren, J., Pitkänen, J., Solberg, S., Wang, Y., Weinacker, H., Hauglin, K.M., Lien, V., Packalén, P., Gobakken, T., Koch, B., Næsset, E., Tokola, T., Maltamo, M., 2012. Comparative testing of single-tree detection algorithms under different types of forest. *Forestry* 85 (1), 27–40.
- Vauhkonen, J., Packalén, P., Malinen, J., Pitkänen, J., Maltamo, M., 2014. Airborne laser scanning based decision support for wood procurement planning. *Scand. J. Forest Res.*, 29 (in press).
- Yu, X., Hyypä, J., Vastaranta, M., Holopainen, M., Viitala, R., 2011. Predicting individual tree attributes from airborne laser point clouds based on the random forests technique. *ISPRS J. Photogramm. Remote Sens.* 66 (1), 28–37.